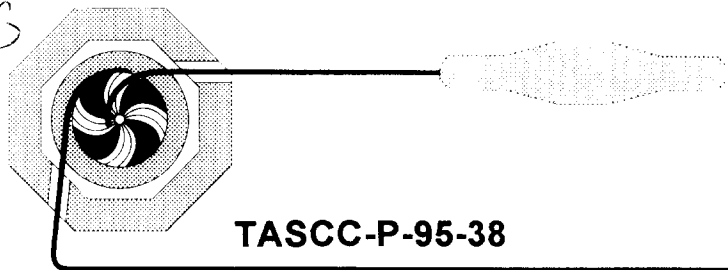


66



TASCC-P-95-38

PREPRINT

tascc

YRAST BAND IN NEUTRON-DEFICIENT ^{115}Xe

**E.S. Paul¹, H.R. Andrews², T.E. Drake³, J. DeGraaf³, V.P. Janzen², S. Pilotte⁴,
D.C. Radford² and D. Ward²**

¹ *Oliver Lodge Laboratory, University of Liverpool,
P.O. Box 147, Liverpool L69 3BX, UK*

² *AECL, Chalk River Laboratories, Chalk River, Ontario, K0J 1J0, Canada*

³ *Department of Physics, University of Toronto, Toronto, Ontario, M5S 1A7, Canada*

⁴ *Department of Physics, University of Ottawa, Ottawa, Ontario, K1N 6N5, Canada*

* Present address: Centre de Recherches Nucléaires, IN2P3-CRNS/ Université Louis Pasteur,
F-67037 Strasbourg Cedex, France

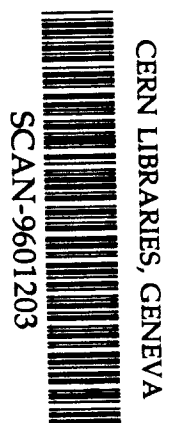
Submitted to Phys. Rev. C
(Brief Reports)

NOTICE

This report is not a formal publication; if it is cited as a reference, the citation should indicate that the report is unpublished. To request copies our E-Mail address is TASCC@CRL.AECL.CA.

Physical and Environmental Sciences
Chalk River Laboratories
Chalk River, ON K0J 1J0 Canada

1995 December



Sw 9606

Yrast band in neutron-deficient ^{115}Xe

E.S. Paul¹, H.R. Andrews², T.E. Drake³, J. DeGraaf³, V.P. Janzen², S. Pilotte^{4*},
D.C. Radford², and D. Ward²

¹ *Oliver Lodge Laboratory, University of Liverpool, PO Box 147, Liverpool L69 3BX, UK*

² *AECL, Chalk River Laboratories, Chalk River, ON, K0J 1J0, Canada*

³ *Department of Physics, University of Toronto, Toronto, ON, M5S 1A7, Canada*

⁴ *Department of Physics, University of Ottawa, Ottawa, ON, K1N 6N5, Canada*

(December 4, 1995)

Abstract

High-spin states have been studied in neutron-deficient ^{115}Xe produced in the $^{60}\text{Ni}(^{58}\text{Ni}, 2\text{pn}\gamma)$ reaction. Transitions have been assigned to ^{115}Xe , for the first time, through their characteristic transition yields with respect to total γ -ray sum-energy and by systematic comparison to neighbouring ^{113}Xe and ^{117}Xe .

PACS numbers: 21.10.Re, 27.60+q, 23.20.Lv.

Typeset using REVTeX

Over the past few years, the study of excited states in neutron-deficient nuclei just above the $Z=50$ shell closure has burgeoned. The extension of the nuclear landscape at moderate to high spins ever closer to the proton dripline has relied on the identification of γ -ray transitions in extremely neutron-deficient nuclei that are populated weakly in fusion-evaporation reactions. Experiments have typically employed γ -ray detection systems coupled to recoil separators with gas ionisation chambers for mass and charge identification; an example is the identification of transitions in the ^{114}Xe nucleus [1]. An alternative approach is to detect the evaporation neutrons, protons and alphas in coincidence with γ -rays, an approach exploited at NORDBALL [2]. For nuclei even closer to the dripline, characteristic charged-particle radioactivity (proton or alpha emission) provides a unique signal for the identification of various nuclei produced. With the advent of the new generation of highly efficient γ -ray spectrometers [3], combined with charged-particle detector arrays, it should be possible to exploit this charged-particle radioactivity to identify nuclei. Indeed, transitions in ^{113}Xe have already been established using this method [4]. Despite the inexorable march towards the dripline, there are still holes in our knowledge, an example being the ^{115}Xe nucleus. In this Brief Report we have established transitions in this nucleus for the first time. Relative γ -ray yields, cross bombardment arguments, comparison to theoretical yields, and systematics of neighbouring odd- A Xe isotopes have been used to assign the transitions to ^{115}Xe .

States in ^{115}Xe were populated with the $^{60}\text{Ni}(^{58}\text{Ni},2\text{pn})^{115}\text{Xe}$ reaction at a bombarding energy of 250 MeV. The ^{58}Ni heavy-ion beam was provided by the Tandem Accelerator Superconducting Cyclotron (TASCC) facility at the Chalk River Laboratories, Canada, while the target consisted of two self-supporting foils of ^{60}Ni , each of nominal thickness $480\ \mu\text{g}/\text{cm}^2$. Coincident γ - γ data were acquired with the 8π spectrometer, consisting of 20

Compton-suppressed HPGe detectors plus a 71-element BGO inner-ball calorimeter, which provides γ -ray sum-energy, H , and fold, K , information. Data were written onto magnetic tape for events in which two or more suppressed HPGe detectors registered in prompt time coincidence with ten or more elements of the inner ball (fold $K \geq 10$). Under this condition, approximately 3.3×10^8 events were recorded to tape. In the off-line analysis of the data for ¹¹⁵Xe (2pn channel), only events with a total sum-energy $H \geq 13.4$ MeV were incremented into a symmetrised $E_\gamma - E_\gamma$ matrix and approximately 50% of the recorded data were replayed into this high- H matrix. The high sum-energy condition greatly suppressed events from the competing 4- and 5-particle evaporation channels which have lower average H and K distributions relative to the 3-particle channels. A second, low- H , matrix was also constructed for events with a total sum-energy in the range $7.0 \leq H \leq 12.2$ MeV.

Analysis of the γ - γ matrices was facilitated by use of the graphical analysis package ESCL8R [6]. Angular-correlation information was obtained from the coincidence data by sorting subsets of the data recorded by HPGe detectors located at specific angles, θ , with respect to the beam axis. A matrix was constructed with data from detectors at $\theta = \pm 37^\circ$ on one axis and detectors at $\theta = \pm 79^\circ$ on the second axis. Angular intensity ratios $I_\gamma(37^\circ, 79^\circ)/I_\gamma(79^\circ, 37^\circ)$ could readily be extracted from this matrix by gating on stretched quadrupole transitions on each axis. These intensity ratios were used to assist in the assignment of transition multipolarities by the method of directional correlation from oriented states (DCO) [7]. For the present geometry, intensity ratios of 1.0 are predicted for a stretched-quadrupole \leftrightarrow stretched-quadrupole correlation and ≈ 0.60 for a stretched-quadrupole \leftrightarrow stretched-dipole (no mixing) correlation [8]. The new transitions assigned to ¹¹⁵Xe from this work are listed in Table I and are shown in the decay scheme presented in Fig. 1, while examples of gated coincidence spectra are shown in Fig. 2. The assignment of

the transitions to ^{115}Xe is now discussed.

The ratios of yields of γ -ray transitions measured in the high- H and low- H coincidence matrices are sensitive to the number of evaporated particles and hence the exit channel; experimental measurements are shown in Table II. It can clearly be seen that values obtained for the new transitions (i.e. ^{115}Xe) are the same as those for the 3p exit channel into ^{115}I . Furthermore, these 3-particle relative yields are twice those obtained for known 4-particle evaporation channels (^{114}I [9], ^{114}Te [10]) and half those for the known 2-particle channel (^{116}Xe [11]). The new transitions can therefore be assigned to a 3-particle evaporation channel with some certainty.

In order to assign the new transitions to a specific exit channel, and hence nucleus, experimental yields, obtained from summing the yields in the low- H and high- H matrices, have been compared to theoretical yields obtained with the ALICE code [12]; the results are shown in Table III normalised to the yield of ^{115}I (3p). The accuracy of statistical evaporation codes applied to extremely neutron-deficient regions is however questionable, tending to underpredict charged-particle emission relative to neutron emission. Indeed, it can be seen in Table III that the relative strength of the new structure is found to be approximately 50% lower than theory for ^{115}Xe (2pn). However, the measured strength of ^{112}I [13] (αpn), which also involves single neutron emission, is similarly found to be approximately 50% of theory. The theoretical yields of two-neutron evaporation channels (^{115}Cs and ^{112}Xe) are an order of magnitude smaller than the 2pn channel, while the yield of the 3n channel (^{115}Ba) is more than two orders of magnitude smaller. These observations strongly suggest that the new transitions may indeed be assigned to the 2pn channel, namely ^{115}Xe .

The level scheme of ^{115}Xe , deduced from the present work, is shown in Fig. 1. The

ordering of the transitions is based on coincidence relationships and relative γ -ray intensities. The level-scheme construction was however severely hampered by contamination from transitions in competing nuclei including ^{114,115}I, ^{112,114}Te, and ¹¹¹Sb; over 300 transitions have been placed in these nuclei from the present data. The only “clean” gates for ¹¹⁵Xe are those for the 415 keV and 767 keV transitions as shown in Fig. 2. The sequence of γ -rays from the 415 keV transition up to the 942 keV transition is well established. The higher, somewhat irregularly spaced transitions are placed according to their extracted intensities, some of which however can be seen to be similar in Table I. It proved possible to measure DCO ratios for most of the transitions and the results are all consistent with stretched E2 character. Hence the relative spin and parity assignments shown in Fig. 1 are good, while the absolute values are taken from systematics of bands in neighbouring nuclides. The new band structure in ¹¹⁵Xe is compared to the yrast bands in neighbouring ¹¹³Xe [4] and ¹¹⁷Xe [14] in Fig. 3, where the smooth systematic behaviour adds further credence to the assignment of the new transitions to ¹¹⁵Xe.

Similar to the neighbouring isotopes, the (11/2⁻) bandhead in Fig. 1 does not represent the ground state of ¹¹⁵Xe. Indeed, studies of γ -rays in coincidence with β -delayed proton emission, i.e. ¹¹⁵Xe $\xrightarrow{\beta}$ ¹¹⁵I \xrightarrow{p} ¹¹⁴Te, suggest a 5/2⁺ ground state for ¹¹⁵Xe [15] with a half-life of approximately 18 s [16]. The ground states in the light odd-A Xe isotopes are based on $\nu d_{5/2}$ or $\nu g_{7/2}$ orbitals, while the yrast bands are based on a low- Ω negative-parity $\nu h_{11/2}$ orbital. The band structure shown in Fig. 1 may be associated with the favoured signature component of a $\nu h_{11/2}$ orbital. The two transitions of energies 893 and 974 keV, shown to the right in Fig. 1, may be $\Delta I=1$ linking transitions depopulating the unfavoured signature component of the $\nu h_{11/2}$ orbital. In this scenario, a large signature splitting would exist with the unfavoured 17/2⁻ state lying above the favoured 19/2⁻ state and the unfavoured 21/2⁻

state lying above the favoured $23/2^-$ state. Such a situation is also observed in ^{117}Xe [14].

Calculations based on the Total Routhian Surface (TRS) formalism [17–19] predict the favoured signature of the $\nu h_{11/2}$ orbital in ^{115}Xe to have a prolate shape with deformation parameters: $\beta_2 \approx 0.215$, $\beta_4 \approx 0.030$, and $\gamma \approx 0^\circ$. Alignment plots for the yrast bands in $^{113,115,117}\text{Xe}$ are presented in Fig. 4, where a variable moment of inertia reference, with Harris parameters [20] $\mathcal{J}_0 = 15\hbar^2\text{MeV}^{-1}$ and $\mathcal{J}_1 = 25\hbar^4\text{MeV}^{-3}$, has been subtracted. These parameters have been adopted from Ref. [14]. The sharp gain in alignment at $\omega \approx 0.45$ MeV/ \hbar in Fig. 4 may be attributed to the rotational alignment of both $\pi h_{11/2}$ and $\nu h_{11/2}$ quasiparticle pairs. A theoretical plot, obtained from the TRS calculations for ^{115}Xe , is also shown for comparison. While the theoretical alignment increases slightly lower in frequency than experiment, two simultaneous alignments of neutron and proton pairs are predicted, with an associated increase in the quadrupole deformation to $\beta_2 \approx 0.250$.

In summary, new transitions have been observed using the $^{60}\text{Ni}(^{58}\text{Ni},2\text{pn})^{115}\text{Xe}$ reaction and assigned to ^{115}Xe , in which no excited states were previously known. The yrast band has been followed up to $I^\pi = (59/2^-)$ and shows evidence for both $\pi h_{11/2}$ and $\nu h_{11/2}$ quasiparticle alignments at high spin.

This work was in part supported by grants from AECL Research, the Natural Sciences and Engineering Research Council of Canada, and the UK Engineering and Physical Science Research Council. The authors are indebted to Dr. R. Wyss and Dr. W. Nazarewicz for providing the TRS cranking codes.

REFERENCES

* Present Address: Centre de Recherches Nucléaires, IN2P3-CRNS/Université Louis Pasteur, F-67037 Strasbourg Cedex, France.

- [1] S.L. Rugari et al., Phys. Rev. C **48**, 2078 (1993).
- [2] A. Johnson et al., Nucl. Phys. **A557**, 401c (1993).
- [3] P.J. Nolan, F.A. Beck, and D.B. Fossan, Annu. Rev. Nucl. Part. Sci. **45**, 561 (1994).
- [4] E.S. Paul et al., Phys. Rev. C **51**, 78 (1995).
- [5] E.S. Paul et al., Phys. Rev. C **50**, 741 (1994).
- [6] D.C. Radford, Nucl. Instrum. and Methods **A361**, 297 (1995).
- [7] K.S. Krane, R.M. Steffen, and R.M. Wheeler, Nuclear Data Tables **A11**, 351 (1973).
- [8] D. Ward et al., Nucl. Phys. **A529**, 315 (1991).
- [9] E.S. Paul, H.R. Andrews, V.P. Janzen, D.C. Radford, D. Ward, T.E. Drake, J. DeGraaf, and S. Pilotte, Phys. Rev. C **52**, 1691 (1995).
- [10] J. Blachot and G. Marguier, Nucl. Data Sheets **60**, 139 (1990).
- [11] J. Blachot and G. Marguier, Nucl. Data Sheets **73**, 81 (1994).
- [12] F. Plasil and M. Blann, Phys. Rev. C **11**, 508 (1975).
- [13] E.S. Paul et al., J. Phys. G **21**, 1001 (1995).
- [14] S. Törmänen et al., Nucl. Phys. **A572**, 417 (1994).
- [15] P. Hornshøj, K. Wilsky, P.G. Hansen, B. Jonson, and O.B. Nielsen, Nucl. Phys. **A599**, 599 (1972); **A599**, 609 (1972).

- [16] P. Hornshøj et al., Phys. Lett. **34B**, 591 (1971).
- [17] R. Wyss, J. Nyberg, A. Johnson, R. Bengtsson, and W. Nazarewicz, Phys. Lett. **B215**, 211 (1988).
- [18] W. Nazarewicz, G.A. Leander, and J. Dudek, Nucl. Phys. **A467**, 437 (1987).
- [19] W. Nazarewicz, R. Wyss, and A. Johnson, Nucl. Phys. **A503**, 285 (1989).
- [20] S.M. Harris, Phys. Rev. **138**, B509 (1965).

TABLES

TABLE I. Properties of the transitions assigned to ¹¹⁵Xe.

E_γ (keV) ^a	I_γ (%) ^b	$\frac{I_\gamma(37^\circ, 79^\circ)}{I_\gamma(79^\circ, 37^\circ)}$ ^c	Multipolarity	Assignment
414.6	100	1.03(6)	E2	(15/2 ⁻ → 11/2 ⁻)
634.7	90	0.96(7)	E2	(19/2 ⁻ → 15/2 ⁻)
767.3	79	0.89(7)	E2	(23/2 ⁻ → 19/2 ⁻)
853.9	54	0.89(7)	E2	(27/2 ⁻ → 23/2 ⁻)
893.0	11			→ (15/2 ⁻)
918.6	41	0.97(7)	E2	(31/2 ⁻ → 27/2 ⁻)
942.4	19	1.03(7)	E2	(39/2 ⁻ → 35/2 ⁻)
952.1	36	0.91(8)	E2	(35/2 ⁻ → 31/2 ⁻)
973.7	17			→ (19/2 ⁻)
1006.8	17	1.10(8)	E2	(43/2 ⁻ → 39/2 ⁻)
1021.0	15	1.09(9)	E2	(47/2 ⁻ → 43/2 ⁻)
1083.8	14	0.94(9)	E2	(51/2 ⁻ → 47/2 ⁻)
1137.3	13	0.99(9)	E2	(55/2 ⁻ → 51/2 ⁻)
1209.4	7		(E2)	(59/2 ⁻ → 55/2 ⁻)
1253.7	10			→ (19/2 ⁻)

^aEnergies are accurate to ±0.3 keV.

^bErrors on the relative intensities are estimated to be less than 10% of the quoted values.

^cThe angular-correlation ratios were obtained from summed spectra gated by the 415 and 767 keV transitions.

TABLE II. Ratios of yields of nuclei measured in the high- H and low- H matrices.

Nucleus	Channel	Relative Yield
^{116}Xe	2p	1.30
^{115}Xe	2pn	0.68
^{115}I	3p	0.69
^{114}I	3pn	0.24
^{114}Te	4p	0.32

TABLE III. Theoretical and experimental relative yields of 3-particle evaporation channels for the $^{58}\text{Ni} + ^{60}\text{Ni}$ reaction at 250 MeV.

Nucleus	Channel	Relative Yield (%)	
		Theory	Experiment ^a
^{115}I	3p	100	100
^{112}Te	α 2p	82	105
^{115}Xe	2pn	32	15
^{112}I	α pn	5.9	3
^{115}Cs	p2n	2.5	b
^{112}Xe	α 2n	2.0	b
^{115}Ba	3n	0.012	b

^aErrors on the experimental yields are estimated to be less than 10% of the quoted values.

^bStates unknown in this nucleus.

FIGURES

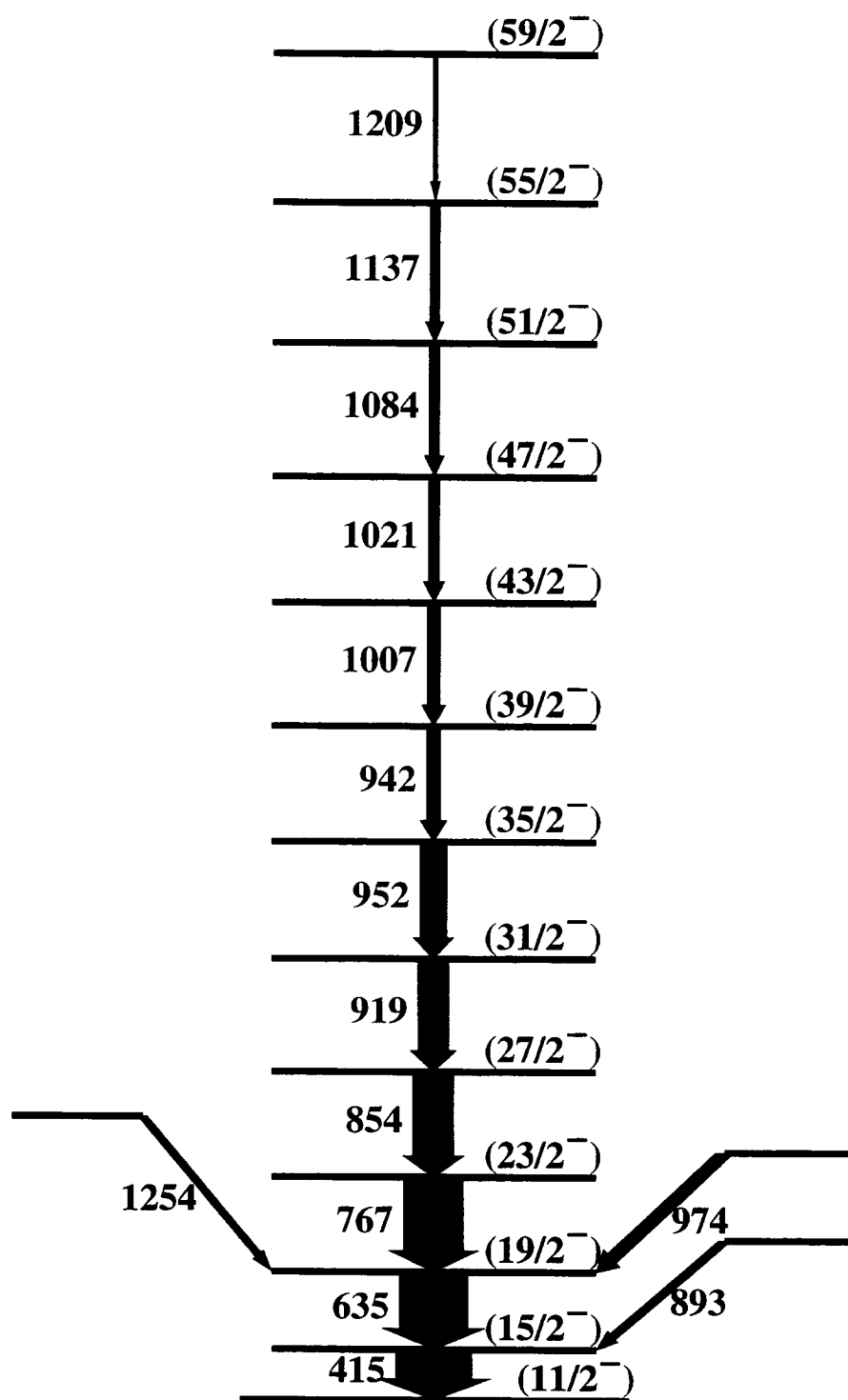
FIG. 1. Level scheme deduced for ^{115}Xe . The transition energies are given in keV and their relative intensities are proportional to the widths of the arrows.

FIG. 2. Examples of gated coincidence spectra. The transitions labelled by their energies in keV have been assigned to ^{115}Xe .

FIG. 3. Systematics of the $\nu h_{11/2}$ yrast bands in odd-A $^{113-117}\text{Xe}$ with assumed spin and parity values.

FIG. 4. Alignment versus rotational frequency for the $\nu h_{11/2}$ bands in odd-A $^{113-117}\text{Xe}$.

^{115}Xe


Fig. 1

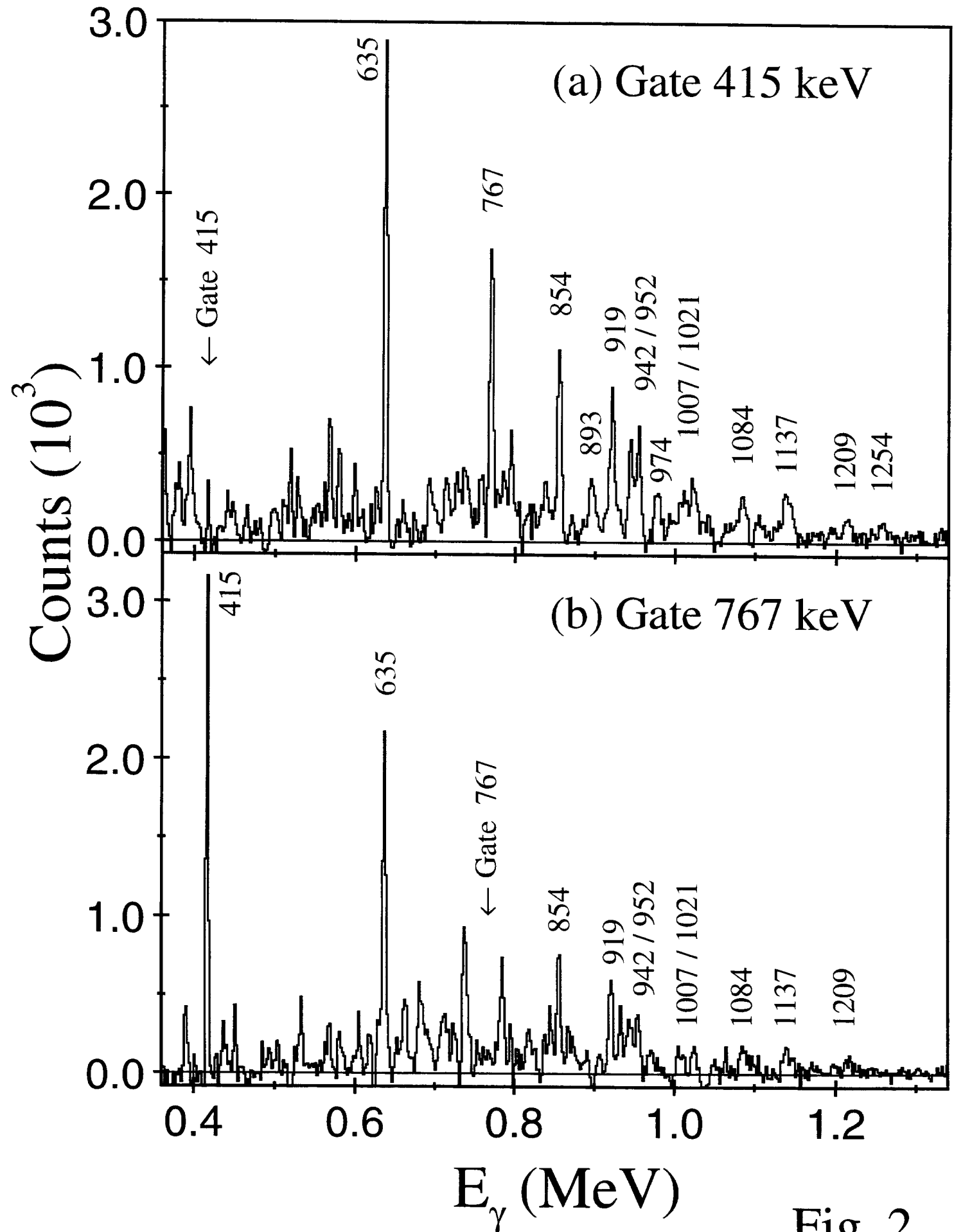


Fig. 2

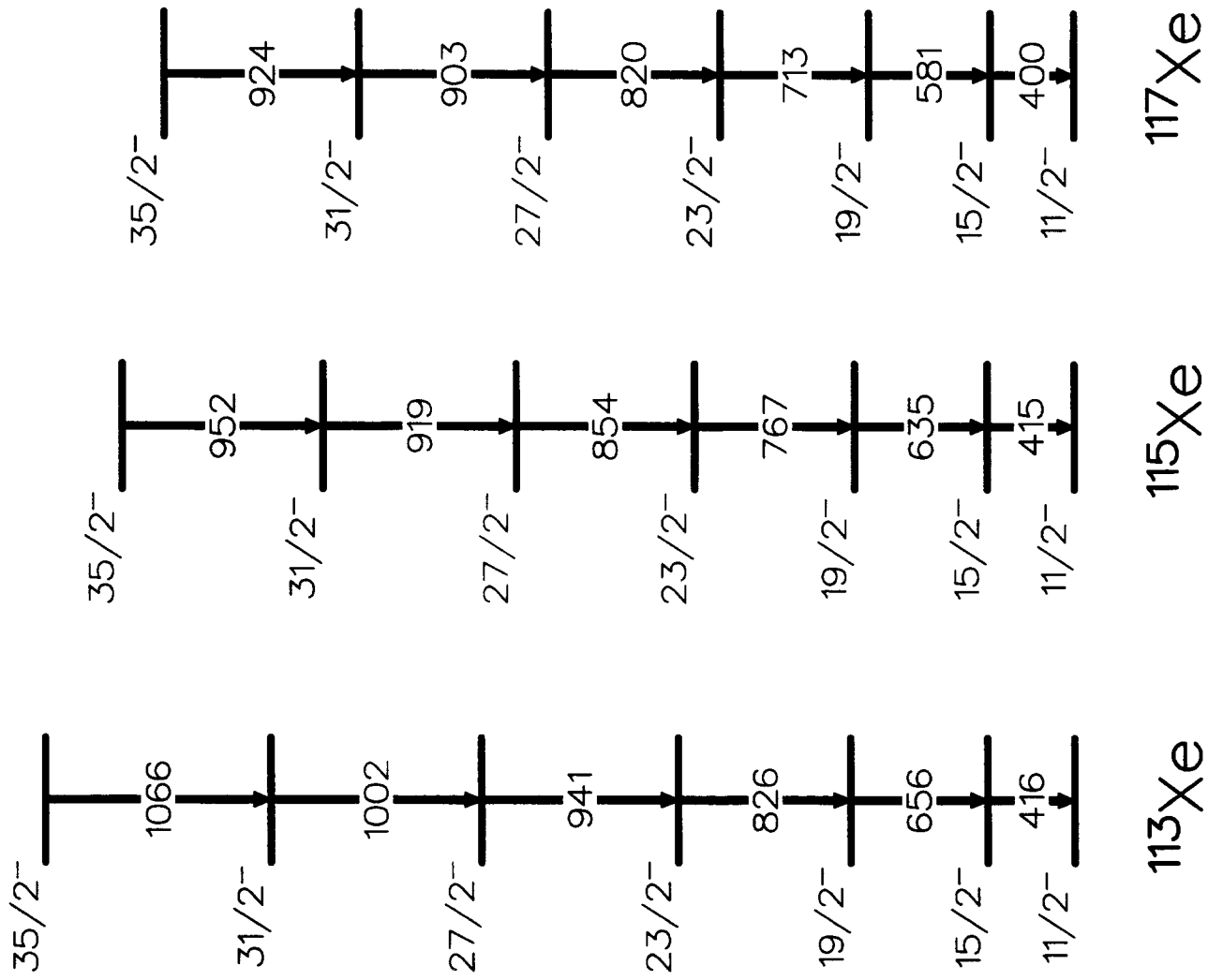


Fig. 3

